Soft Matter

Physical Aging and Compressed Exponential Behaviors in a Model Soft Colloidal System

Journal:	*Soft Matter*
Manuscript ID	SM-ART-10-2018-002042.R3
Article Type:	Paper
Date Submitted by the Author:	03-Feb-2019
Complete List of Authors:	Li, Qi; Texas Tech Univ, Chemical Engineering Peng, Xiaoguang; Texas Tech Univ, Chemical Engineering McKenna, Gregory; Texas Tech Univ, Chemical Engineering

Physical Aging and Compressed Exponential Behaviors in a Model Soft Colloidal System

Qi Li, Xiaoguang Peng, and Gregory B. McKenna
Department of Chemical Engineering, Texas Tech University, Lubbock TX 79409

{February 6, 2019}

ABSTRACT

Diffusing wave spectroscopy (DWS)-based micro-rheology has been used in different optical geometries (backscattering and transmission) as well as different sample thicknesses in order to probe system dynamics at different length scales [Pine DJ, Weitz DA, Zhu JX, Herbolzheimer E. *J. Phys. France,* 1990, 51(18), 2101-2127.]. Previous study from this lab [Li Q, Peng X, McKenna GB. *Soft Matter,* 2017, 13(7), 1396-1404.] indicates the DWS-based micro-rheology observes the system non-equilibrium behaviors differently from macro-rheology. The object of the present work was to further explore the non-equilibrium dynamics and to address the range of utility of DWS as a micro-rheological method. A thermo-sensitive core-shell colloidal system was investigated both during aging and subsequent to aging into a metastable equilibrium state using temperature-jump induced volume fraction-jump experiments. We find that in the non-equilibrium state, significant differences in the measured dynamics are observed for the different geometries and length scales. Compressed exponential relaxations for the autocorrelation function $g_2(t)$ were observed for large length scales. However, upon converting the $g_2(t)$ data to the mean square displacement (MSD), such differences with length scale diminished and the long-time MSD behavior was consistent with diffusive behavior. These observations in the non-equilibrium behaviors for different length scales leads to questioning of some interpretations in the current field of light scattering-based micro-rheology and provides a

possibility to interrogate the aging mechanisms in colloidal glasses from a broader perspective than normally considered in measurements of $g_2(t)$ using DWS-based micro-rheology.

INTRODUCTION

Soft colloidal systems have attracted significant attention as model systems from which to gain insight into the glass transition and physical aging phenomena [1,2,3]. The particle interpenetration or compression due to the particle softness [1,4,5,6] results in high volume fractions and enables investigation of these materials in the deep glassy state [7]. Current theories related to the physical aging of soft colloidal systems include caging theory [8], mode-coupling theory (MCT) [9,10,11], soft glassy rheology model (SGR) [12,13], the self-consistent generalized Langevin equation (SCGLE) theory [14,15], as well as activated hopping in the framework of a nonlinear Langevin equation (NLE) theory [16,17]. Caging theory describes the relaxation process as arising from particle escape from local confinement or "cages" formed by the surrounding particles [8]. The relaxation process from MCT's perspective considers relaxations of different Fourier components, which are related to the coupling between density fluctuations [9]. The SGR model from Sollich and coworkers [12] constructs an energy landscape with many energy minima and the activation process for relaxation denotes particles overcoming the different energy barriers related to the energy landscape. The SCGLE theory of Medina-Noyola and co-workers [14,15] depicts a homogeneous system and approaches the aging behaviors from the structure factors. The NLE approach proposed by Schweizer and co-workers [16,17] describes a trapping and a barrier hopping process for a type of activated glassy dynamics in a heterogeneous system. Experimentally, soft colloidal systems show their own aging signatures compared with hard-sphere colloidal systems and molecular glasses. The soft

interaction and overpacking at high volume fractions result in a competition between thermal energies and elastic energies [18,19,20], which affect the equilibrium aging dynamics: the "super-Arrhenius" type of prediction of the α-relaxation time vs. volume fraction disappears, and concentration dependence of the dynamics turns towards a plateau-like region at high concentrations [2,21,22]. In the non-equilibrium regime, soft colloidal systems show stronger cooperative motion than hard sphere colloids [23], and dynamic heterogeneity has been reported to play an important role during aging [24,25]. Furthermore, key findings from our lab [2] include a faster aging rate as measured with DWS-based micro-rheology compared with macro-rheology, as well as the decoupling of the α-relaxation time and the equilibration time.

Micro-rheology has proven to be a powerful tool in constructing phase diagrams [26,27], studying flow behaviors [28], and measuring the viscoelastic properties of soft colloidal systems [29,30]. Among the micro-rheological methods, diffusing wave spectroscopy (DWS) is widely used and the well-developed multiple scattering theory enables DWS to extend the traditional dynamic light scattering (DLS) to concentrated systems, allowing one to probe the system at length scales smaller than the wave length of light [30,31,32]. In the context of soft colloidal systems, DWS-based micro-rheology is thought to capture the equilibrium dynamics in colloids approaching their glass transition concentrations [1,2,33] and measure the rheological properties over a wide frequency range [27]. In these prior works, DWS-based micro-rheology was reported to show good agreement with macro-rheology [33]. However, when the system was out of equilibrium, viz., in aging experiments, it was found that the response in DWS resulted in extremely high aging rates (shift rates) compared to comparable macroscopic rheological measurements, i.e., DWS seems to probe the system differently compared to macro-rheology [2].

In the present work, DWS-based micro-rheology was used to investigate the aging behaviors of a model polystyrene (PS)-poly(N-isopropylacrylamide) (PNIPAM)/poly(acrylic acid) (PS-PNIPAM/AA) core-shell thermo-sensitive soft colloidal system at different length scales. The PNIPAM-based soft colloidal systems have been intensely studied for almost twenty years [34]. Experimental efforts on synthesis [35,36], characterization [37,38], softness effects [1,13,20,22,39], as well as aging dynamics [2,13,40,41,42,43,44] provide a solid fundamental understanding of these systems and motivate further studies exploiting these systems. Previous studies from our laboratory on the dynamics of a PS-PNIPAM/AA soft colloidal system found that in equilibrium, good agreement was achieved between DWS-based micro-rheology and macro-rheological measurements [33] through the generalized Stokes-Einstein relationship [45]. Moreover, results from DWS on samples aged for long times to achieve equilibrium show that the α-relaxation time as a function of volume fraction deviates from the VFT-type prediction and a "soft jamming" regime is observed [2]. Such deviations were also observed by Archer and coworkers [21] in PEG-silica nanoparticle suspensions, as well as by Philippe et al. [22] in PNIPAM microgels and in a dispersion of silica particle with surface charges.

In terms of non-equilibrium behaviors, previous work from our group by Di et al. [40] and Peng et al. [43] studied the Kovacs structural recovery (aging) signatures [46] in soft colloidal dispersions (pure PNIPAM and PS-PNIPAM/AA system, respectively). They found that in both systems, unlike the behavior seen by Kovacs in molecular glasses where timescales increase dramatically with decreasing temperature, the time to reach equilibrium for the colloidal systems showed very weak volume fraction dependence. Furthermore, a weak asymmetry of approach behavior was observed, suggesting a weak nonlinearity of the system. Additionally, unlike the molecular glasses and rheological measurements on a similar PNIPAM-based system,

there was an almost vanished memory effect in the DWS measurements. Some, but not all, of these Kovacs signatures were found in the calculations from Banik and McKenna [47] using the TNM-KAHR model for Kovacs-like isochoric conditions, which are suggested to be similar in concept to iso-volume fraction conditions investigated in colloids. In addition to the Kovacs signatures, Li et al. [2] observed high shift rates (up to 4) during aging using DWS micro-rheology. This compares with shift rates obtained from macro-rheology for a similar system of less than unity [48].

To summarize, in prior work, it has been found that, in the non-equilibrium state, DWS in backscattering mode showed a behavior different from that measured by macroscopic rheological measurements. The present work is motivated by the hypothesis that the reasons for the observed differences are related to the fact that the DWS probes the system at short length scales, i.e., is a micro-rheological measurement. Here we use temperature-jump induced volume fraction-jumps using a PS-PNIPAM/AA core shell system and probe the response using DWS in different geometries (backscattering and transmission) and different transmission lengths (sample size), from which we have been able to probe length scales from 1.3 nm to 36.0 nm. The results show that the scattering geometry and length scale affect the results, consistent with the above hypothesis. In addition, further information is obtained upon conversion of the data to mean squared displacement as a function of time.

EXPERIMENTAL

Materials

The soft colloidal system investigated in this study was a thermosensitive PS-PNIPAM/AA core-shell latex. The synthesis procedure and characterization have been described in prior works [33,42,43]. The mass concentration for the colloidal sample used in this work was

16.0 wt% PS-PNIPAM/AA in nanowater (Barnstead Nanopure Infinity System, by Thermo Scientific). The hydrodynamic diameters were determined by dynamic light scattering (Nanotrac 250, Macrotrac, Inc.) equipped with a temperature controlled ($\pm$ 0.1°C) water bath. Crystallization was prevented by using a 25% polydispersity in particle size [49,50]. Figure 1 shows the hydrodynamic diameter as a function of temperature [43] for the PS-PNIPAM/AA particles. The temperature range for the present work was from 25 °C to 30.2 °C, and the diameter of the particles shows a linear relationship within this temperature range, as seen in Figure 1. The effective volume fraction ϕ_{eff} for the sample at different temperatures was determined from[33,40,51,52]: $\phi_{eff}(T) = \phi_{eff,collapsed}[^{D(T)}/_{D_{collapsed}}]^3$, where $\phi_{eff}(T)$

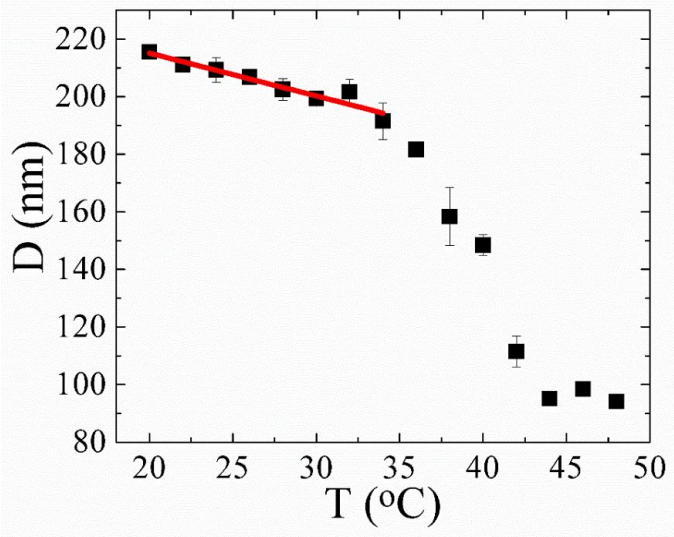

FIG.1. Dependence of the hydrodynamic diameter of the PS-PNIPAM/AA particles on temperature. The line represents a linear fit of $D(T) = 244.85 - 1.4869T$, where T is in degrees Celsius (After Peng and McKenna [43]. Copyright 2016. American Physical Society, with permission.

and $\phi_{eff,collapsed}$ denote the effective volume fraction ϕ_{eff} at temperature T and in the collapsed state, respectively. $D(T)$ and $D_{collapsed}$ represent the diameters of the particles at temperature T and in the collapsed state at high temperature (above 45 °C), respectively. $\phi_{eff,collapsed}$ is calculated from the following equation: [53]

$$\phi_{eff,collapsed} = \frac{m_{colloid}/\rho_{colloid}}{\frac{m_{colloid}}{\rho_{colloid}} + m_{solvent}/\rho_{solvent}} \quad (1)$$

where m and ρ denote the mass and density, respectively, for colloid or solvent. The density for our PS-PNIPAM/AA sample is 1.071 g/ml. The $\phi_{eff,collapsed}$ value for the current 16.0 wt% PS-PNIPAM/AA sample is 0.151. Because of the complex nature of soft colloidal interactions, the determination of the effective volume fraction is known to be problematic [54]. The role of the electrostatic layer and different soft interactions in the calculation of effective volume fraction are still not clear [5,54,55,56]. Here we use $\phi_{eff,collapsed}$ to determine the effective volume fraction using particle diameter and composition, in consideration of the relatively small electrostatic layer in the particles used [35,57]. The effective volume fraction in this study is larger than unity because of the interpenetration and/or compression between particles [1,4,5,6].

Diffusing Wave Spectroscopy (DWS)

Diffusing wave spectroscopy (DWS) [30,32] experiments with two different geometries were performed in this study, including backscattering and transmission. For these two different geometries, different length scale information can be extracted [30,58]. The length scales probed for different DWS geometries are defined as [30,58,59]

$$l_B^2 = 1/k_0^2\left(\frac{z_0}{l^*} - \frac{2}{3}\right)^2 \quad (2)$$

$$l_{Tr}^2 = \left(\frac{l^*}{k_0 L}\right)^2 \quad (3)$$

For the backscattering geometry, the length scale, l_B, is related to the wave number, $k_0 = 2\pi/\lambda$, the penetration depth, z_0 [60], and the light transport mean free path, l^*. The length scale, l_{Tr}, in the transmission geometry is a function of l^*, k_0^2, as well as the sample thickness, L.

The scattering mean free path l^* is concentration dependent for colloidal samples. Here, for each volume fraction, l^* was obtained by comparing the transmitted light intensity with that of a reference latex suspension sample (Polybead® Microspheres 0.35 μm, Polysciences, Inc.) with a fixed concentration (2.6 wt%) and a known l^* [61]:

$$\frac{\mathrm{T}}{T_S} = \frac{l^*(1+\frac{4l_S^*}{3\,L})}{l_S^*(1+\frac{4l^*}{3\,L})} \tag{4}$$

where T and T_S are transmission light intensity for the sample and for the reference sample, respectively. l_S^* is the scattering mean free path for the reference sample ($l_S^* = 93.7$ μm). For the backscattering geometry, a sample thickness of 1 cm was used. For the transmission geometry, sample thicknesses of 1 mm, 2 mm, and 1 cm were used. This allows probing different length scales because the characteristic length scale for transmission geometry, l_{Tr}, is related to sample thickness (Equation (3)). Different sample thicknesses were achieved by using sample cuvettes (from LSinstruments Inc.) with different internal dimension, which sets the sample thickness. A rotatable polarizer is placed before the CCD camera to increase the signal to noise ratio for measurements done in transmission geometry [62]. For different geometries and concentrations, the scattering mean free path l^* was calculated from Equation (4) and ranged from 198.6 μm to 291.4 μm. At the temperatures and sample thicknesses examined in this work, the diffusion approximation limit ($\mathrm{L}/l^* > 3$) was satisfied [61]. The length scale probed for each sample size and DWS geometry are given in Table 1:

Table 1: DWS Length Scales and l* for Different Experimental Conditions

	Temperature / °C	*Backscattering*	*Transmission*			*l* for Transmission geometry / μm*
Sample thickness		1 cm	1 cm	2 mm	1 mm	

Length scale / nm	30.2	1.3	2.9	14.7	29.4	291.4
Length scale / nm	29.0	1.3	2.5	12.8	25.5	253.4
Length scale / nm	28.7	1.3	2.0	10.0	20.0	198.6

With multi-speckle analysis, aging dynamics of the current soft colloidal sample was monitored using DWS through the intensity autocorrelation function $g_2(t)$ for both backscattering and transmission geometries [63]:

$$g_2(t) = \frac{\langle I(t_0)I(t_0+t)\rangle}{\langle I(t_0)\rangle\langle I(t_0+t)\rangle} \quad (5)$$

where *I* denotes the intensity of light at one pixel and the <> brackets indicate the average over pixels on the CCD chip. For the current experimental setup, a coherent laser source was used with a wavelength of 633 nm. A CCD camera (Basler acA640-120uc), at a speed of 120 frames per second, was used to collect the scattered light.

RESULTS & DISCUSSION

Time-Aging Time Superpositions

Aging behaviors were observed following temperature down-jump induced volume fraction up-jumps on the current thermo-responsive soft colloidal dispersion. All the measurements started when the system reaches the testing temperature, which defines zero time. For DWS measurements in the backscattering geometry, the intensity autocorrelation function $g_2(t)$ was determined for different aging times t_w, as shown in Figure 2(a). After the temperature jump, with increasing aging time, the $g_2(t)$ curves shift toward longer time until they start to overlap, indicating a metastable equilibrium state is reached for the current temperature jump. Similar to previous work on the same colloidal system [2,33,42,43], horizontal shifting of these $g_2(t)$ curves leads to a master curve construction as shown in

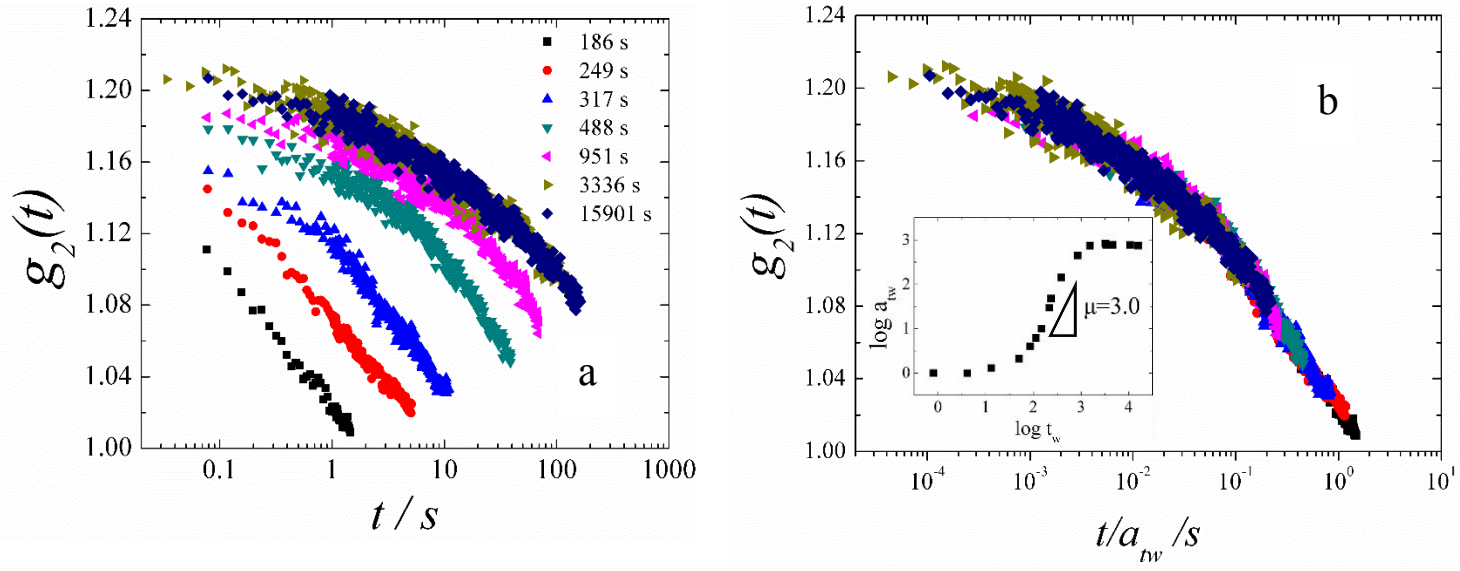

FIG.2. (**a**) Intensity autocorrelation function $g_2(t)$ from backscattering measurements by DWS for a 16.0 wt% PS-PNIPAM/AA latex at different waiting times t_w subsequent to a temperature down-jump from an equilibrium state at 30.2°C to an out-of-equilibrium state at 28.7 °C. These correspond to an effective volume fraction ϕ_{eff} up-jump from 1.449 to 1.498. (**b**) Master curve formed by applying time-aging time superposition to the $g_2(t)$ versus t/a_{tw} using simple horizontal shifting. Vertical shifting was not required. Inset presents the $\log_{10} a_{tw}$ vs. $\log_{10} t_w$, showing a slope in the power-law aging regime that gives a shift rate of $\mu \approx 3.0$.

Figure 2(b). Hence, time-aging time superposition is valid for the current PS-PNIPAM/AA colloidal system in the backscattering DWS geometry [46]. From shifting all the $g_2(t)$ curves to construct the master curve in Figure 2(b), the shift rate μ can be defined [48] and calculated from the double logarithmic slope of scaled relaxation time [64] (shift factor $a_{tw} = \tau(t_w)/\tau(t_{w,ref})$) and aging time t_w in the power law regime ($\mu = dlog_{10}a_{tw}/dlog_{10}t_w$). From the Figure 2(b) insert we see that $\mu \approx 3.0$. This high shift rate value is in agreement with previous DWS results [2] but differs significantly from the response obtained in macro-rheological measurements on a similar system after volume fraction jumps ($\mu < 1$) [43] or from DWS measurements on a hard sphere colloidal system (pure repulsive polystyrene beads) after shear melting ($\mu = 1$) [65]. It is also much greater than the value obtained in molecular glasses, generally $\mu \leq 1$ [48].

DWS geometry and sample thickness are another two factors that can affect the intensity autocorrelation function $g_2(t)$ [30,58]. Therefore, it is of interest to examine the colloidal system using transmission geometry and different sample thicknesses. Figure 3(a) shows the $g_2(t)$ curves for a transmission geometry (sample thickness 1 cm) and for different aging times after

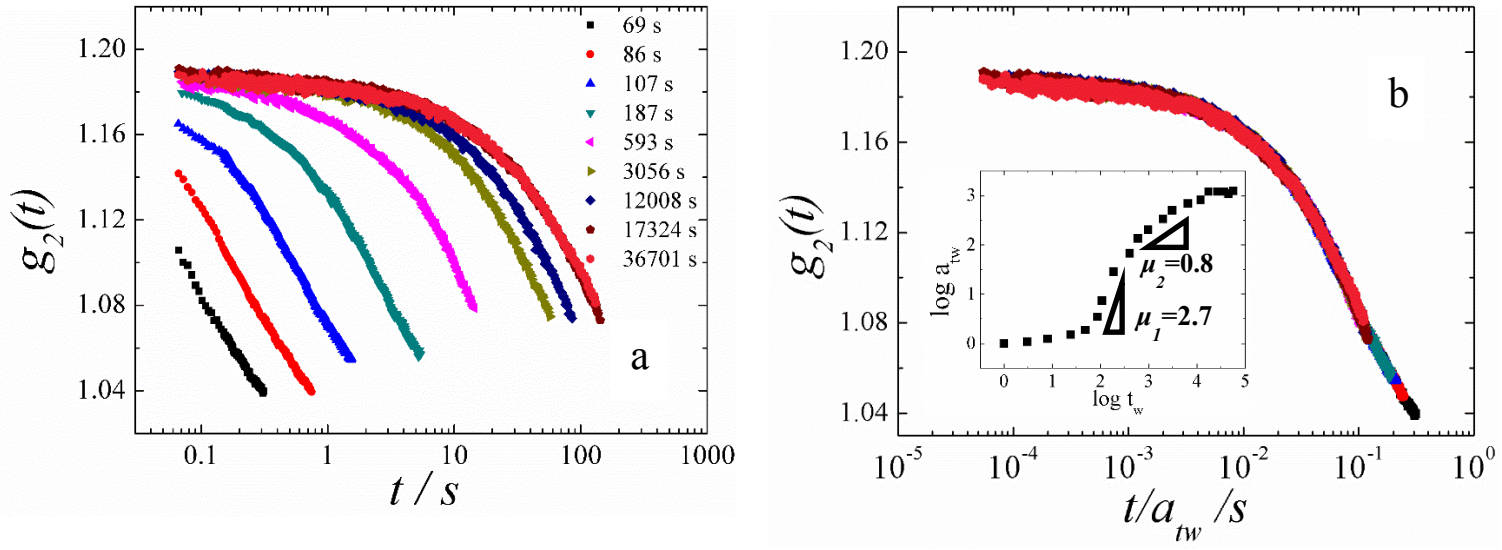

FIG.3. (**a**) DWS measurements of the intensity autocorrelation function $g_2(t)$ for 16.0 wt% PS-PNIPAM/AA colloidal dispersion in transmission geometry (sample thickness 1.0 cm) at different waiting time t_w with the same temperature down-jump experiment from an equilibrium state at a volume fraction of 1.449 to an out-of-equilibrium state at a volume fraction of 1.498 as backscattering measurements. (**b**) Time-aging time superposition: master curve of $g_2(t)$ versus t/a_{tw} after a simple horizontal shifting. No vertical shifts were applied. (inset) the logarithm of the time-aging time superposition shift factor $\log_{10} a_{tw}$ as a function of the logarithm of the aging time $\log_{10} t_w$, with two shift rates $\mu_1 = 2.7$ and $\mu_2 = 0.8$.

the same temperature jump as in Figure 2, from an equilibrium state at a volume fraction of 1.449 to a non-equilibrium state at a volume fraction of 1.498. It is clear to see that, for the same experimental process, the DWS geometry plays an important role in determining the shape of the g_2(t) curves. Despite the difference in geometry and the shape of the $g_2(t)$ curves, time-aging time superposition is also valid in the transmission measurements. Figure 3(b) presents the master curve after horizontal shifting of the $g_2(t)$ curves towards short time. In transmission geometry, more sample thicknesses were tested, including 1 cm, 2 mm, and 1 mm. The time-

aging time superposition holds for all length scales tested for our current PS-PNIPAM/AA samples.

Compressed Exponential Decays

To illustrate the length scale effect on the intensity autocorrelation function $g_2(t)$, g_2 curves for different length scales are plotted versus time in Figure 4. The g_2 curves here are all in the equilibrium state at a volume fraction of 1.498, with *L/l** values vary from 5.0 to 50.3 for the different length scale measurements (see Table 1). From Figure 4, the intensity autocorrelation function $g_2(t)$ shows three regimes in the time range investigated: a short-time regime where the

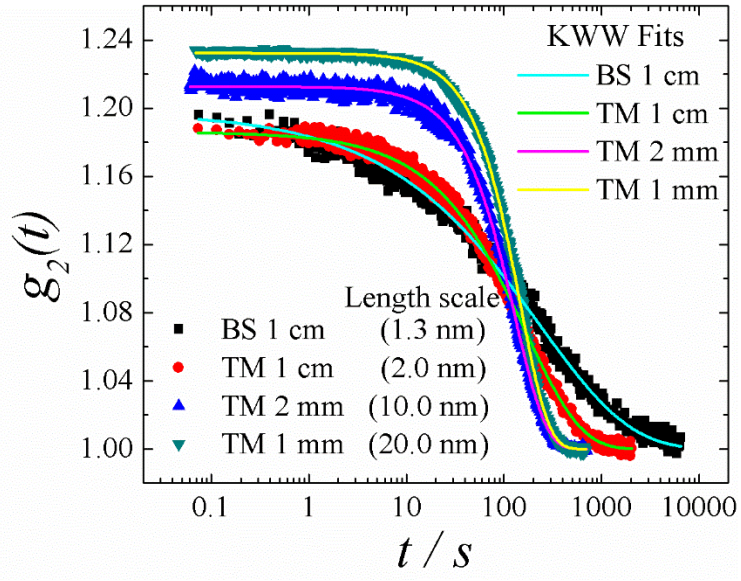

FIG.4. The intensity autocorrelation function $g_2(t)$ for backscattering (black squares) and transmission geometries for different sample thicknesses (1 cm: red circles; 2 mm: blue up-triangles; 1 mm: cyan down-triangles). Lines through data are from KWW fits. The data are for samples aged into the equilibrium state after a concentration-jump from $\phi_{eff} = 1.449$ to $\phi_{eff} = 1.498$.

decay of $g_2(t)$ is weak; a fast decay regime where $g_2(t)$ decays rapidly over time and does so more rapidly as sample thickness decreases (or the probed length scale increases); and a long-time decorrelation regime. At short times (< 10 s), the backscattering $g_2(t)$ curve shows no

obvious short-time plateau-like regime while for the $g_2(t)$ curves obtained in the transmission geometry, the short-time plateau-like regime is clear and covers an increasingly wide range of time with increasing length scale. For the rapid decay regime, the $g_2(t)$ curves from the transmission measurements decay faster than does that from the backscattering counterpart. With decreasing sample thickness (increasing length scale), the decay accelerates. The back-scattering regime, which represents the shortest length scale probed, takes the longest time to completely decorrelate while the decorrelation times for the transmission measurements are shorter than for the backscattering and longest for the largest transmission geometry which relates to the shortest length scale probed in this geometry.

To further investigate the decay curves, the Kohlrausch-Williams-Watt (KWW) function [66,67] $g_2(t) = 1 + Aexp[-2\left(\frac{t}{\tau}\right)^{\beta}]$ was used to fit the $g_2(t)$ curves. Here τ is a characteristic relaxation time, and β is a shape parameter. A compressed exponential ($\beta > 1$) behavior is observed in the transmission geometry for the 2 mm and 1 mm sample thicknesses, indicating the system observed by DWS relaxes faster than a simple exponential function. The four β values for these four $g_2(t)$ curves are 0.44, 0.77, 1.27, and 1.60 from left to right in Figure 4(a). Such compressed exponential behavior has been reported in many light scattering or X-ray scattering-related experimental methods for metallic glasses [68,69,70], polymer gels [71,72,73,74], concentrated colloidal systems [22,75,76,77], as well as some other glass forming systems with probe particles [78,79]. This unusual super-diffusive behavior is thought to be related to the relaxation of internal stress and a ballistic-like dynamics in this regime, proposed by Cipelletti et al. [72,80], as well as Bouchaud and Pitard [81]. To examine this idea, the system mean square displacement (MSD) $\langle \Delta r^2(t) \rangle$ was calculated for each $g_2(t)$ curve. The MSD calculation results

are presented in Figure 5. For the backscattering geometry, an analytical expression was used [30,82]:

$$g_2(t) - 1 = exp\left[-2\gamma\sqrt{k_0^2\langle\Delta r^2(t)\rangle + a} + 2\gamma\sqrt{a}\right] \quad (6)$$

In Equation (6), γ quantifies the low-order scattering, *i.e.* the coupling of the incident light to the turbid sample. For this sample, we follow Cardinaux et al. [82] (for a concentrated giant micelle solution) and take $\gamma = 1.9$, a is a parameter characterizing the deviation of the current geometry from that of an idealized semi-infinite slab, *i.e.* the photon loss along the multi-scattering path. This correction factor depends only on geometry and we again follow Cardinaux et al. [82] and take $a = 0.0035$. $k_0 = 2\pi/\lambda$ is the wave number. For the transmission geometry, The MSD was determined by numerical inversion of the equations relating the autocorrelation function with the mean square displacement and instrument parameters as given in [30]:

$$g_2(t) - 1 = \left\{ \frac{(\frac{L}{l^*} + \frac{4}{3})\langle\sqrt{k_0^2\Delta r^2(t)}\rangle}{sinh\left[(\frac{L}{l^*} + \frac{4}{3})\langle\sqrt{k_0^2\Delta r^2(t)}\rangle\right]} \right\}^2 \quad (7)$$

The two methods of MSD calculation (Equations 6 and 7) were validated by using DWS measurements on two relatively dilute PS-PNIPAM/AA samples having mass fractions of 1.0 wt% and 0.4 wt%, corresponding to effective volume fractions of 10.8% and 4.3%. For each measurement, the value of L/l^* was tuned to the match the values used in the present work. The calculated MSDs for both geometries increase linearly with time, indicating Brownian behavior. The diffusion coefficient D were obtained from the calculated MSD curves from the relation $\langle\Delta r^2(t)\rangle = 6Dt$ and it was found that D=$9.49 \times 10^{-13}\mathrm{m}^2\mathrm{s}^{-1}$ and $1.08 \times 10^{-12}\mathrm{m}^2\mathrm{s}^{-1}$, for the 1.0 wt% and 0.4 wt% samples, respectively. From independent measurements we determined the viscosities for the 1.0 wt% and 0.4 wt% to be $1.07 \times 10^{-3}Pa$ and $9.41 \times 10^{-4}Pa$. From the

Stokes-Einstein equation ($D = \frac{k_B T}{6\pi\eta r}$) we can determine D=$9.50 \times 10^{-13} m^2 s^{-1}$(1.0 wt%) and $1.08 \times 10^{-12} m^2 s^{-1}$ (0.4 wt %), which are in consistent with results from MSD curves. Such agreements indicate that the parameters used in Equation 6 and Equation 7 are appropriate for the current study. Apart from these checks in the relatively dilute colloidal systems, it is worth mentioning that the accuracy of $g_2(t)$ or MSD analysis (Equations 6 and 7) in complex fluids remains an important area of investigation. For example, in a shaving cream foam system, local bubble rearrangement dynamics were not captured in the $g_2(t)$ and MSD determinations [83,84,85]. Similarly, in concentrated colloidal systems, the effects of dynamic heterogeneity remain a subject of study when $g_2(t)$ or MSD are investigated [77]. However, we emphasize that in this part of the present work, the $g_2(t)$ or the calculated MSD responses are all for a system aged into equilibrium. Also, in our previous work, DWS-based micro-rheology shows good agreements with macro-rheological measurements when the samples have been aged into the equilibrium state [33], supporting the use $g_2(t)$ or MSD analysis in concentrated colloidal systems.

In Figure 5(a), the calculated MSD curves for the different length-scales are very similar in contrast with the sharp differences observed among the length-scale dependent $g_2(t)$ curves. This implies that DWS from different length-scale measurements observe similar particle motions. Despite that the MSD data are close from different geometries, differences are also observed. The subtle differences in MSD are thought to arise from the differences in the *L/l** values for different scattering geometries. While all of the curves seem to asymptote towards a diffusive behavior, the MSDs calculated from the two stretched exponential $g_2(t)$ do so more slowly than do the two compressed exponential curves. At the same time, the shapes of the MSD curves in the mid-portion of the plot in Figure 5(a) show a sharper change towards the

diffusive regime for the compressed exponential curves of Figure 4 than do the data corresponding to the stretched exponential curves. Hence, it appears from these data that the compressed exponential decay seen in the $g_2(t)$ curves is caused by a narrower transition of the MSD curve towards the diffusive regime rather than by a super diffusive MSD behavior. No super-diffusive motion in the MSD curves (slope >1) was observed even though the $g_2(t)$ curves gave compressed exponential behaviors. We remark that from our current evidence, super-diffusive motion is not the reason for the compressed exponential behavior observed in the $g_2(t)$ curves, and if there is internal stress relaxation, it is only related to diffusive or sub-diffusive motions of the particles. Furthermore, any internal stress relaxation has only subtle effects on the structural relaxation processes [86]. From the internal stress relaxation theory, the residual stress in the system gives rise to local displacements of the particles. Since the cage-escape progress is

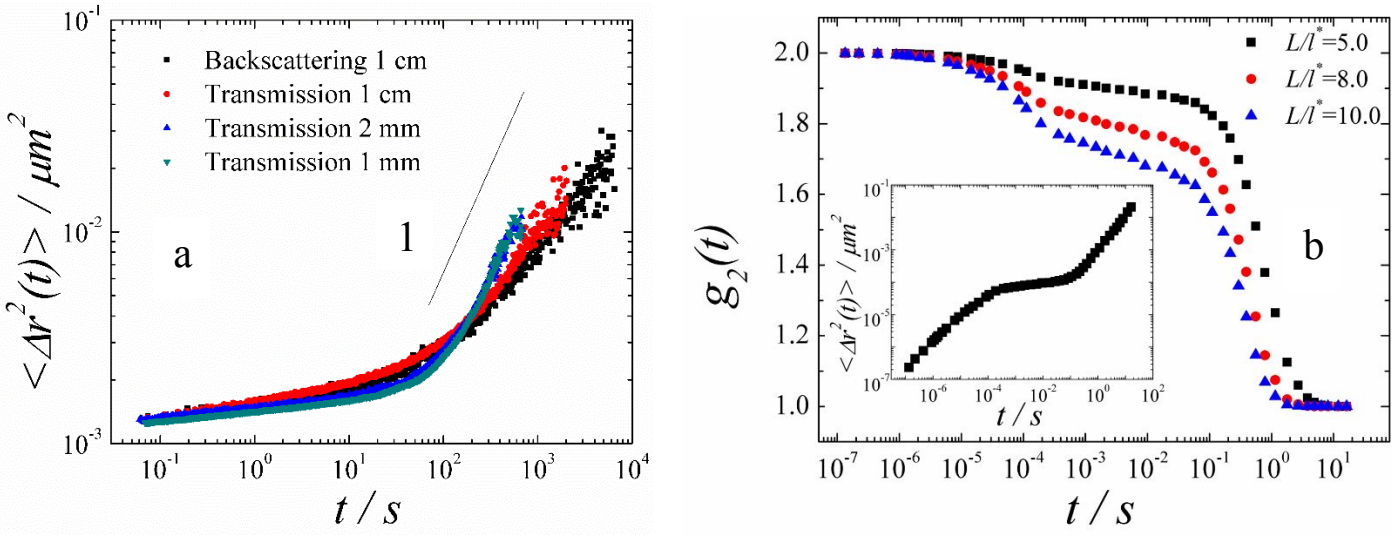

FIG.5. (a) Mean square displacement $< \Delta r^2(t) >$ versus time for different length scale measurements after volume fraction up-jump from 1.449 to 1.498. The dashed line shows the diffusive limit of a slope of 1. (b) Calculated $g_2(t)$ from a self-constructed typical MSD. The MSD plot is shown in the insert. Different values of L/l^* were used, as indicated in the figure.

sub-diffusive due to hydrodynamic interactions [71], this internal stress may turn the long-time sub-diffusive motion into diffusive-like motion but seems not related to the compressed

exponential behaviors. From our perspective, the observed compressed exponential behaviors in the g_2 curves result from the way in which $g_2(t)$ is measured being dependent on mode (transmission or backscattering) and length-scale probed (sample thickness): in the theory of light scattering, beyond equation (5), the intensity autocorrelation function $g_2(t)$ can also be expressed in terms of the distribution of path lengths:

$$\sqrt{g_2(t)-1} = g_1(t) = \int_0^\infty P(s) e^{-2\left(\frac{t}{\tau_0}\right)\left(\frac{s}{l^*}\right)} ds. \quad (8)$$

where $g_1(t)$ is the electric field autocorrelation function and can be related to the intensity autocorrelation function $g_2(t)$ through the Siegert relation [30]. $P(s)$ is a distribution function for light travelling a path length of *s* and is dependent on the light scattering geometry. For different length scale measurements, the distribution functions $P(s)$ are also different, hence, the shapes of the $g_2(t)$ functions for different length scales are distinct [31,82,87,88]. Here we remark that since the coherent factor $g^{-1} \approx \left[(k_0 l^*)(k_0 L)\right]^{-1}$ is much smaller than unity (in all cases $< 10^{-7}$), we can then neglect the coherent contribution of the light paths (particle comparative motions) [30], and Equation 8 is valid in the current conditions. Such a length-scale dependent $g_2(t)$ function and length-scale insensitive MSD function have been reported previously for giant micelle solutions (Scheffold and co-workers [82]; Munch and co-workers [88]) and from granular flow studies on spherical glass beads of size ~100 μm (Menon and Durian [89]). In these works, the shape parameter β for different geometry measurements on a same system was reported to be different by as much as a factor of 1.5 [82].

Beyond the basic $g_2(t)$ –to-MSD conversions, we made further attempts to examine the compressed exponential decay problem. Part of the analysis can be seen in Figure 5(b) which shows the $g_2(t)$ curves back-calculated from a self-constructed MSD curve that does not show

any super-diffusive behavior. Different shapes of $g_2(t)$ curves were obtained upon using different L/l^* values in our calculations. These MSD data were fit to the KWW function for values of L/l^* of 5.0, 8.0 and 10.0 (within the diffusion approximation limit for DWS where L/l^* should be larger than 3 [61]). The corresponding KWW shape parameters β are 1.23, 1.20, and 1.17, i.e., they are indicative of compressed exponential behavior. The results from Figure 5(b) further support our ideas and demonstrate an important point that in DWS, the compressed exponential can be obtained from an MSD response that shows normal long-time diffusive behavior and is not necessarily related to super-diffusive (ballistic-like) motion.

Apart from the problematic direct use of $g_2(t)$ scattering measurements to interpret system dynamics, the anomalous diffusion process and the stretched Gaussian (compressed exponential) behavior have been studied in some other respects. From molecular dynamics simulations by Del Gado and co-workers [90,91], as well as Douglas and co-workers [92,93] on a colloidal gel and a polymer-grafted nanoparticle suspension, clustering dynamics (or induced clustering) inside the sample, can stretch the Gaussian distribution and results in a compressed exponential behavior of the autocorrelation function. One thing that needs to be mentioned here comes from the work of Douglas and co-workers [92] on a polymer-grafted nanoparticle suspension. Under the assumption of an ideal Brownian diffusion, their calculated MSD from the compressed exponential intermediate scattering function shows super-diffusive behavior in the long-time limit (with a slope of 1.9). On the other hand, Del Gado and co-workers [90,91] did not observe any super-diffusive behavior in their directly-measured MSD in the simulation results. We remark that during the MSD calculation, the ideal Brownian diffusion assumption is questionable in the studied non-ideal colloidal system. Some more relevant results were reported in other glass-forming liquids: Morishita [94] and Seo et al. [95] studied liquid silicon and

trehalose, respectively, and found the particle interaction as well as intra-molecular structure (which may be related to the clustering dynamics) are responsible for the compressed exponential behavior observed in intermediate scattering functions or $g_2(t)$ curves. Moreover, from a theoretical view, particle persistent motion can be an important factor in this type of fast dynamics and is thought to be undetectable in the MSD [96,97]. In present work, we show that the observation of a compressed exponential in the autocorrelation functions does seem consistent with the observation of normal diffusive behavior as determined from the calculated MSD response. More evidence is needed to fully resolve this question.

Shift Factors

Despite the problems in the intensity autocorrelation function, the shift factor (as discussed above in Figure 2) may still be a good method to study the aging dynamics. Figure 2(a) and 2(b) show the time-aging time superposition of $g_2(t)$ curves, the shift factors obtained are $a_{tw,g2(t)}$. A similar definition can be applied to the MSD curves. Figure 6(a) shows the MSD curves during aging after a volume fraction jump from 1.449 to 1.488 for transmission geometry

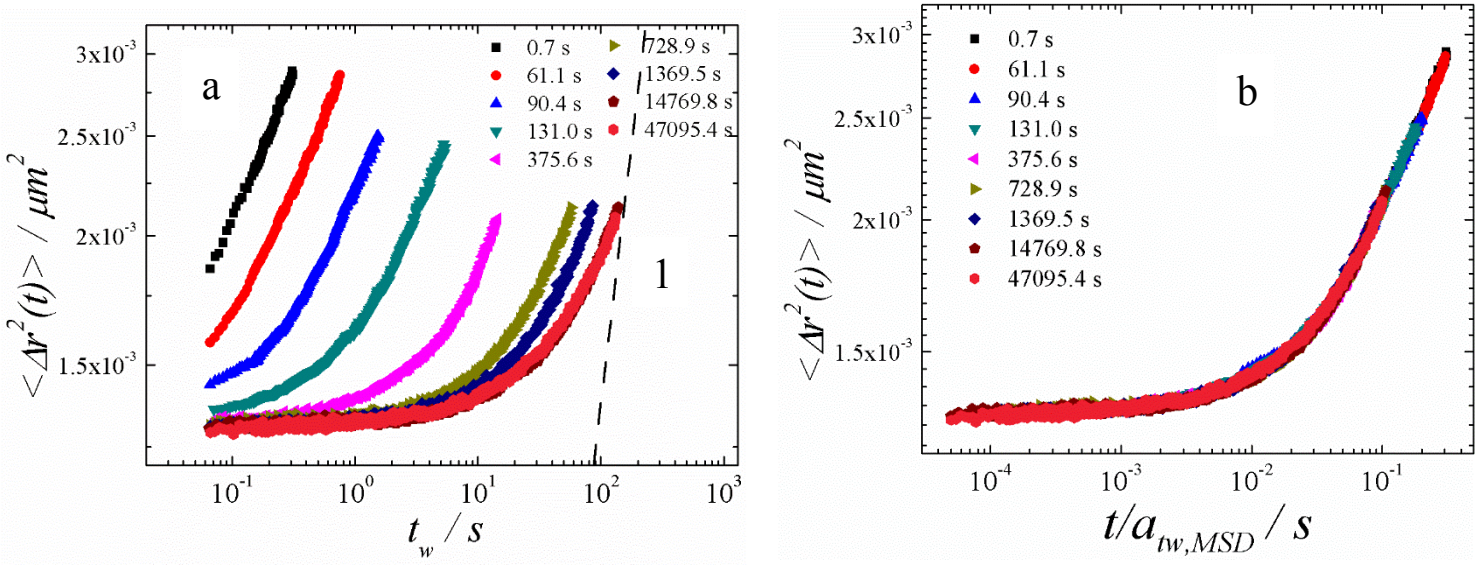

FIG.6. (**a**) DWS transmission measurements (sample thickness 1 cm) of the mean square displacement $<\Delta r^2(t)>$ for 16.0 wt% PS-PNIPAM/AA latex at different waiting time t_w after temperature down-jump from an equilibrium state

at 30.2°C to an out-of-equilibrium state at 29.0 °C. These conditions correspond to an effective volume fraction ϕ_{eff} up-jump from 1.449 to 1.488. (**b**) Master curve obtained after applying time-aging time superposition to the $<\Delta r^2(t)>$ versus $t/a_{tw,MSD}$ data of Figure 6(a). Only simple horizontal shifting without vertical shifts was applied.

with a sample thickness of 1 cm. Similar to the $g_2(t)$ curves, with increasing aging time, the MSD curves shift toward longer time until they start to overlap, indicating a metastable equilibrium state is reached for the current volume fraction jump. The time-aging time superposition master curves can be constructed via simple horizontal shifts and are shown in Figure 6(b).

Figure 7(a) and Figure 7(b) show the shift factors $a_{tw,g2(t)}$ and $a_{tw,MSD}$ as a function of waiting time after $g_2(t)$ curve shifting and MSD curve shifting, respectively. The shift factor $a_{tw,g2(t)}$ and $a_{tw,MSD}$ both show a sigmoidal dependence [98] on waiting time for all the DWS geometries and sample thicknesses, as discovered in our prior research in backscattering measurements [2]: from a flat short aging time regime, to a rapid increasing intermediate aging

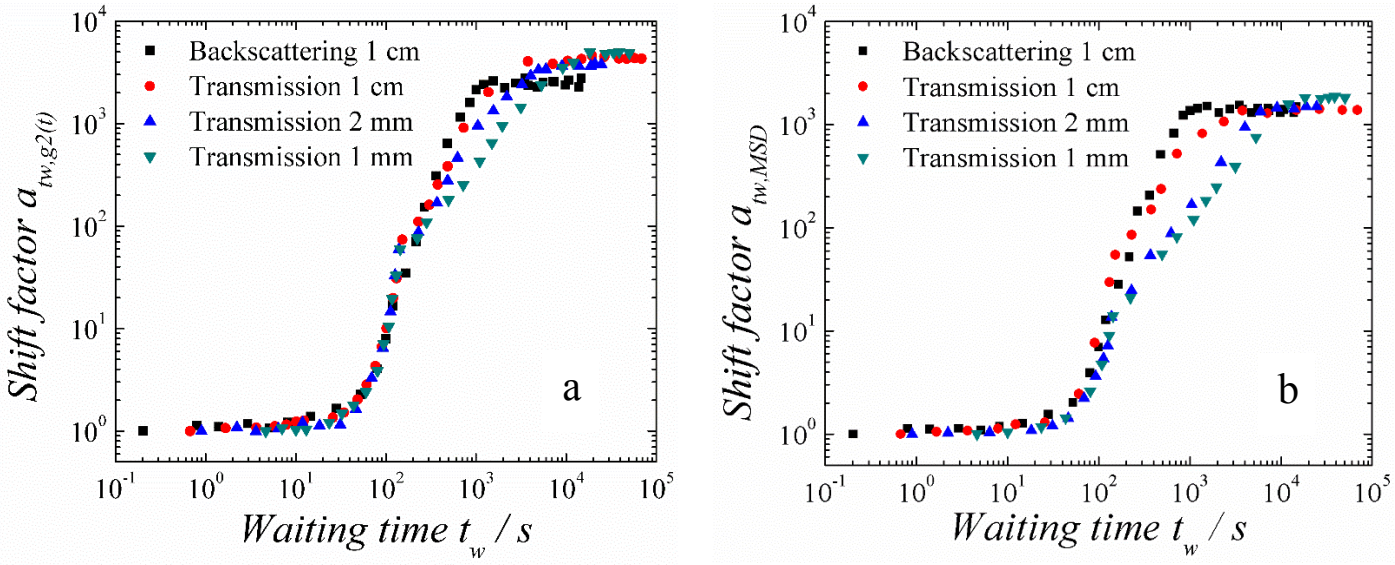

FIG.7. (**a**) Shift factor $a_{tw,g2(t)}$ as a function of waiting time t_w for backscattering and transmission geometry with different sample thicknesses (1 cm, 2 mm, and 1 mm) after volume fraction up-jump from an equilibrium state at a 1.449 to a non-equilibrium state at a 1.488. (**b**) Shift factor $a_{tw,MSD}$ as a function of waiting time t_w for backscattering and transmission geometry with different sample thicknesses (1 cm, 2 mm, and 1 mm) after volume fraction up-jump from an equilibrium state at a 1.449 to a non-equilibrium state at a 1.488.

time regime, to a final long aging time plateau. However, for the different DWS geometries and sample thicknesses, differences in this sigmoidal dependence were observed. In the short aging time regime, the corresponding a_{tw} of this almost 'flat' region depends upon DWS geometry. For the transmission measurements, this region overlaps for the different sample thicknesses (length scales), indicating similar short-time dynamics observed for different length scale measurements. On the other hand, backscattering measurements seem to probe slightly different short aging time dynamics immediately after the temperature down-jump (volume fraction up-jump) compared to the transmission measurements. Possible reasons for this difference come from the different path length distributions $P(s)$ (introduced in Equation (6)) probed by backscattering and transmission DWS geometries [31].

After the short aging time regime, the $a_{tw,g2(t)}$ and $a_{tw,MSD}$ curves for different geometries and sample thicknesses start to overlap at the beginning of the intermediate aging time regime. At around 200 s, the a_{tw} curves start to deviate for the different DWS geometries and sample thicknesses, and the intermediate aging time regime splits into two parts for the transmission results. With increasing length scale, the aging rate slows down after the deviation point. Similar observations of two parts in the intermediate aging time regime were reported by the SCGLE model calculations of homogeneously aging colloidal systems, including both soft colloids and hard-sphere colloidal systems, from Medina-Noyola and coworkers [99,100]. Experimentally, if we carefully revisit the data, this type of two stages inside the intermediate aging time regime is seen in previous studies on the same colloidal system (13.4 wt%) [2] following temperature down-jumps with backscattering DWS measurements. However, the length scale effect was not investigated in either the SCGLE model calculations or previous experimental findings.

The underlying physics of these two stages in the intermediate aging time regime is still unclear. However, a few points can be proposed in the current situation: first, this type of two stages has been clearly observed experimentally only in deep glassy states (highly packed states) for soft colloidal systems. The effective soft interaction or the softness, a hidden structure factor [101], is thought to play an important role for this observation. Second, in the second part of the intermediate aging time regime, the aging rate deviates more from the early time trend as lenthg scale increases. It is of interest to see that the deviations seem to all occur around $t_w = 100\ s$. Third, from the SCGLE model calculations, this intermediate aging regime was also found to be non-smooth and split into two stages for both soft and hard-sphere colloidal systems [99,100]. This prediction from the homogeneous SCGLE model [14,15] provides evidence that these two stages are not related to the dynamic heterogeneity of the system.

Despite the fact that the two shift factors $a_{tw,g2(t)}$ and $a_{tw,MSD}$ share similarities, differences are also observed. Figure 8(a) and 8(b) show comparisons between $a_{tw,g2(t)}$ and $a_{tw,MSD}$ in two difference length scale measurements. The four curves are taken from Figure 7(a) and 7(b). From Figure 8(a), it is clear to see that these two types of shift factors give slightly different aging dynamics, especially in the intermediate aging regime and long-time aging regime. In these regimes, the MSD shift factor $a_{tw,MSD}$ is always smaller than the $g_2(t)$ shift factor under the same experimental conditions, indicating that the $g_2(t)$ curves seem to capture different information than MSD does. However, with increasing length-scale (decreasing sample thickness), the differences between $a_{tw,g2(t)}$ and $a_{tw,MSD}$ curves in the intermediate aging regime become larger. Such idea of a length scale dependent difference can be supported by Figure 8(b), where the comparison happens at the smallest length scale (from backscattering measurements). In Figure 8(b), the two shift factors show good agreement until the long-time equilibrium plateau regime.

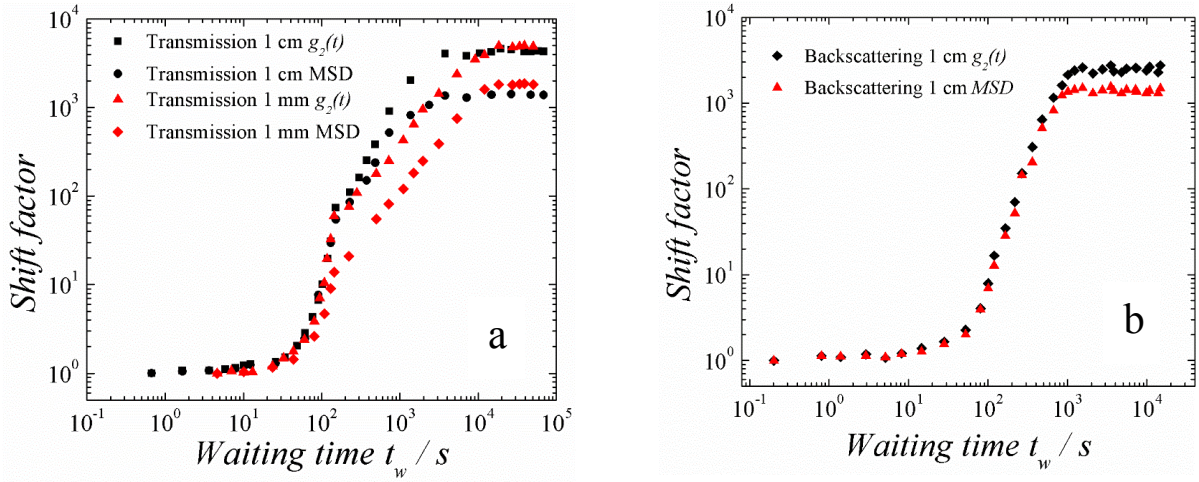

FIG.8. (**a**) Shift factors $a_{tw,g2(t)}$ and $a_{tw,MSD}$ as a function of waiting time t_w from transmission measurements of two different sample thicknesses (1 cm and 1 mm) after volume fraction up-jump from an equilibrium state at a 1.449 to a non-equilibrium state at a 1.488. (**b**) Shift factors $a_{tw,g2(t)}$ and $a_{tw,MSD}$ as a function of waiting time t_w from backscattering measurements of two different sample thicknesses (1 cm and 1 mm) after volume fraction up-jump from an equilibrium state at a 1.449 to a non-equilibrium state at a 1.488.

We remark that such differences in the second stage of the intermediate aging regime are related to the emergence of compressed exponential decay of the $g_2(t)$ curves. As a result, the compressed exponential decay from the problematic $g_2(t)$ curves is affecting the observed aging dynamics. Further work is needed to construct a correct aging dynamics from the DWS experiments.

SUMMARY AND CONCLUSIONS

The dynamics of a 16.0 wt% PS-PNIPAM/AA soft thermo-sensitive colloidal system were studied with DWS-based micro-rheology after temperature down-jump induced volume fraction up-jump experiments. Both equilibrium dynamics and the effects of aging on the dynamics were investigated. Different DWS geometries (backscattering and transmission) and sample thicknesses were also studied to investigate the length-scale effects on the colloid dynamics and physical aging process.

From the DWS experiments one determines the intensity autocorrelation function $g_2(t)$ and it is found that there is a strong length-scale dependence of the behavior. Of particular interest is the result for the equilibrium dynamics in which we observed a short-time regime where the decay of $g_2(t)$ is very slow and which becomes more developed as the length scale probed in the measurements increases. In the transmission measurements for the largest length-scales probed, compressed exponential decays were observed. The $g_2(t)$ curves for both the stretched and compressed exponential cases were converted to mean square displacement (MSD). In all MSD curves, no "super-diffusive" behavior was observed, indicating the compressed exponential decay is not necessarily related to a "super-diffusive" behavior, and does not represent the true relaxation response of the system. Rather, the compressed exponential decays of the $g_2(t)$ curves seem to be the result of the relationships between $g_2(t)$ and MSD for the different scattering geometries in the (light) scattering experiments and not to internal stress relaxation [71,80]. Other factors such as particle clustering dynamics [90,91,92,93], particle interactions [94,95], particle persistent motion [96,97], or even temperature gradient induced convections in the system [102], have been proposed to play important roles in the observed compressed exponential behavior of $g_2(t)$.

Looking at the aging (non-equilibrium) response, since time-aging time superposition is valid for all length-scale measurements in the current soft colloidal system, shift factors $a_{tw,g2(t)}$ and $a_{tw,MSD}$ were then compared based on the $g_2(t)$ curves and MSD curves, respectively. Beyond a sigmoidal aging time dependence of $a_{tw,g2(t)}$ and $a_{tw,MSD}$, the intermediate aging time regime (power law regime) was found to split into two parts for large length scale measurements (all from transmission geometry) and the aging rate slows down in the second part with increasing length scale. When carefully comparing these two types of shift factors, differences

were found in the second stage of the intermediate aging regime as well as the long-time equilibrium plateau regime, and the difference becomes larger with increasing length scale. This implies that the problematic compressed exponential decay observed in the $g_2(t)$ curves also subtly affects the observed aging dynamics.

ACKNOWLEDGEMENTS

We thank Dongjie Chen from our research group for his viscosity measurements, J. Galen Wang and R. N. Zia for their valuable discussions on light scattering, the National Science Foundation (Grants No. CBET 1133279 and No. CBET 1506072) and the John R. Bradford Endowment at Texas Tech University, each for partial support of this work.

REFERENCES

[1] Mattsson J, Wyss HM, Fernandez-Nieves A, Miyazaki K, Hu Z, Reichman DR, Weitz DA. Soft colloids make strong glasses. *Nature.* 2009, 462(7269), 83-86.

[2] Li Q, Peng X, McKenna GB. Long-term aging behaviors in a model soft colloidal system. *Soft Matter.* 2017, 13(7), 1396-1404.

[3] Hunter GL, Weeks ER. The physics of the colloidal glass transition. *Rep. Prog. Phys.* 2012, 75(6), 066501.

[4] Gasser U, Hyatt JS, Lietor-Santos J-J, Herman ES, Lyon LA, Fernandez-Nieves A. Form factor of pNIPAM microgels in overpacked states. *J. Chem. Phys.* 2014, 141(3), 034901.

[5] Mohanty PS, Nöjd S, van Gruijthuijsen K, Crassous JJ, Obiols-Rabasa M, Schweins R, Stradner A, Schurtenberger P. Interpenetration of polymeric microgels at ultrahigh densities. *Sci. Rep.* 2017, 7(1), 1487.

[6] Conley GM, Aebischer P, Nöjd S, Schurtenberger P, Scheffold F. Jamming and overpacking fuzzy microgels: Deformation, interpenetration, and compression. *Sci. Adv.* 2017, 3(10), e1700969.

[7] McKenna GB, Simon SL. 50th Anniversary Perspective: Challenges in the Dynamics and Kinetics of

Glass-Forming Polymers. *Macromolecules.* 2017, 50(17), 6333-6361.

[8] Weeks ER, Weitz DA. Subdiffusion and the cage effect studied near the colloidal glass transition. *Chem. Phys.* 2002, 284(1-2), 361-367.

[9] Götze W, Sjögren L. Relaxation processes in supercooled liquids. *Rep. Prog. Phys.* 1992, 55(3), 241.

[10] Sciortino F, Tartaglia P. Glassy colloidal systems. *Adv. Phys.* 2005, 54(6-7), 471-524.

[11] Kobayashi M, Sasaki A. Electrophoretic mobility of latex spheres in mixture solutions containing mono and divalent counter ions. *Surf. A Physicochem. Eng. Asp.* 2014, 440, 74-78.

[12] Sollich P, Lequeux F, Hébraud P, Cates ME. Rheology of soft glassy materials. *Phys. Rev. Lett.* 1997, 78(10), 2020.

[13] Purnomo EH, van den Ende D, Mellema J, Mugele F. Rheological properties of aging thermosensitive suspensions. *Phys. Rev. E.* 2007, 76(2), 021404.

[14] Guevara-Rodríguez FJ, Medina-Noyola M. Dynamic equivalence between soft-and hard-core Brownian fluids. *Phys. Rev. E.* 2003, 68(1), 011405.

[15] Ramírez-González PE, Medina-Noyola M. Glass transition in soft-sphere dispersions. *J. Phys. Condens. Matter.* 2009, 21(7), 075101.

[16] Schweizer KS, Saltzman EJ. Entropic barriers, activated hopping, and the glass transition in colloidal suspensions. *J. Chem. Phys.* 2003, 119(2), 1181-1196.

[17] Yang J, Schweizer KS. Glassy dynamics and mechanical response in dense fluids of soft repulsive spheres. I. Activated relaxation, kinetic vitrification, and fragility. *J. Chem. Phys.* 2011, 134(20), 204908.

[18] Jacquin H, Berthier L. Anomalous structural evolution of soft particles: equilibrium liquid state theory. *Soft Matter.* 2010, 6(13), 2970-2974.

[19] Ikeda A, Berthier L, Sollich P. Disentangling glass and jamming physics in the rheology of soft materials. *Soft Matter.* 2013, 9(32), 7669-7683.

[20] Di Lorenzo F, Seiffert S. Counter-effect of Brownian and elastic forces on the liquid-to-solid transition of microgel suspensions. *Soft Matter.* 2015, 11(26), 5235-5245.

[21] Wen YH, Schaefer JL, Archer LA. Dynamics and rheology of soft colloidal glasses. *ACS Macro Lett.* 2015, 4(1), 119-123.

[22] Philippe AM, Truzzolillo D, Galvan-Myoshi J, Dieudonné-George P, Trappe V, Berthier L, Cipelletti L. Glass transition of soft colloids. *Phys. Rev. E.* 2018, 97(4), 040601.

[23] Rahmani Y, van der Vaart K, van Dam B, Hu Z, Chikkadi V, Schall P. Dynamic heterogeneity in hard and soft sphere colloidal glasses. *Soft Matter.* 2012, 8(15), 4264-4270.

[24] Cipelletti L, Weeks ER, in *Dynamical Heterogeneities in Glasses, Colloids, and Granular Media*. Oxford Univ. Press, Oxford. pp. 1-46, 2011.

[25] Jabbari-Farouji S, Zargar R, Wegdam GH, Bonn D. Dynamical heterogeneity in aging colloidal glasses of Laponite. *Soft Matter.* 2012, 8(20), 5507-5512.

[26] Meng Z, Cho JK, Breedveld V, Lyon LA. Physical aging and phase behavior of multiresponsive microgel colloidal dispersions. *J. Phys. Chem. B.* 2009, 113(14), 4590-4599.

[27] Furst EM, Squires TM, *Microrheology*, Oxford, 2017.

[28] Squires TM, Mason TG. Fluid mechanics of microrheology. *Annu. Rev. Fluid Mech.* 2010, 42(1), 413-438.

[29] Liu J, Gardel ML, Kroy K, Frey E, Hoffman BD, Crocker JC, Bausch AR, Weitz DA. Microrheology probes length scale dependent rheology. *Phys. Rev. Lett*. 2006, 96(11), 118104.

[30] Weitz DA, Pine DJ, in *Dynamic Light Scattering: The Method and Some Applications*. Oxford Univ. Press, Oxford. pp. 652-720, 1993.

[31] Pine DJ, Weitz DA, Chaikin PM, Herbolzheimer E. Diffusing wave spectroscopy. *Phys. Rev. Lett.* 1988, 60(12), 1134.

[32] Maret G. Diffusing-wave spectroscopy. *Curr. Opin. Coll. Int. Sci.* 1997, 2(3), 251-257.

[33] Di X, Peng X, McKenna GB. Dynamics of a thermo-responsive microgel colloid near to the glass transition. *J. Chem. Phys.* 2014, 140(5), 054903.

[34] Yunker PJ, Chen K, Gratale MD, Lohr MA, Still T, Yodh AG. Physics in ordered and disordered colloidal matter composed of poly (N-isopropylacrylamide) microgel particles. *Rep. Prog. Phys.* 2014, 77(5), 056601.

[35] Dingenouts N, Norhausen C, Ballauff M. Observation of the volume transition in thermosensitive core-shell latex particles by small-angle x-ray scattering. *Macromolecules.* 1998, 31(25), 8912-8917.

[36] Kim JH, Ballauff M. The volume transition in thermosensitive core-shell latex particles containing charged groups. *Colloid Polym. Sci.* 1999, 277(12), 1210-1214.

[37] Stieger M, Pedersen JS, Lindner P, Richtering W. Are thermoresponsive microgels model systems for concentrated colloidal suspensions? A rheology and small-angle neutron scattering study. *Langmuir.* 2004, 20(17), 7283-7292.

[38] Crassous JJ, Ballauff M, Drechsler M, Schmidt J, Talmon Y. Imaging the volume transition in thermosensitive core-shell particles by cryo-transmission electron microscopy. *Langmuir.* 2006, 22(6), 2403-2406.

[39] Le Grand A, Petekidis G. Effects of particle softness on the rheology and yielding of colloidal glasses. *Rheol. Acta.* 2008, 47(5-6), 579-590.

[40] Di X, Win KZ, McKenna GB, Narita T, Lequeux F, Pullela SR, Cheng Z. Signatures of structural recovery in colloidal glasses. *Phys. Rev. Lett.* 2011, 106(9), 095701.

[41] van den Ende D, Purnomo EH, Duits MHG, Richtering W, Mugele F. Aging in dense suspensions of soft thermosensitive microgel particles studied with particle-tracking microrheology. *Phys. Rev. E.* 2010, 81(1), 011404.

[42] Peng X, McKenna GB. Comparison of the physical aging behavior of a colloidal glass after shear melting

and concentration jumps. *Phys. Rev. E.* 2014, 90(5), 050301.

[43] Peng X, McKenna GB. Physical aging and structural recovery in a colloidal glass subjected to volume-fraction jump conditions. *Phys. Rev. E*. 2016, 93(4), 042603.

[44] Peng X, Wang JG, Li Q, Chen D, Zia RN, McKenna GB. Exploring the validity of time-concentration superposition in glassy colloids: Experiments and simulations. *Phys. Rev. E.* 2018, 98(6), 062602.

[45] Einstein A, in *Investigation on the Theory of Brownian Movement*, Dover, New York, 1956.

[46] Kovacs AJ. Transition vitreuse dans les polymères amorphes. Etude phénoménologique. *Fortschr. Hochpolym. Forsch.* 1964, 3(1), 394-507.

[47] Banik S, McKenna GB. Isochoric structural recovery in molecular glasses and its analog in colloidal glasses. *Phys. Rev. E.* 2018, 97(6), 062601.

[48] Struik LCE, *Physical Aging in Amorphous Polymers and Other Materials*, Elsevier, Oxford, 1978.

[49] Siebenbürger M, Fuchs M, Winter HH, Ballauff M. Viscoelasticity and shear flow of concentrated, noncrystallizing colloidal suspensions: Comparison with mode-coupling theory. *J. Rheol.* 2009, 53(3), 707-726.

[50] Ballauff M, Brader JM, Egelhaaf SU, Fuchs M, Horbach J, Koumakis N, Krüger M, Laurati M, Mutch KJ, Petekidis G, Siebenbürger M, Voigtmann T, Zausch J. Residual stresses in glasses. *Phys. Rev. Lett.* 2013, 110(21), 215701.

[51] Senff H, Richtering W, Norhausen C, Weiss A, Ballauff M. Rheology of a Temperature Sensitive Core-Shell Latex. *Langmuir.* 1999, 15(1), 102-106.

[52] Deike I, Ballauff M, Willenbacher N, Weiss A. Rheology of thermosensitive latex particles including the high-frequency limit. *J. Rheol.* 2001, 45(3), 709-720.

[53] Eckert T, Richering W. Thermodynamic and hydrodynamic interaction in concentrated microgel suspensions: Hard or soft sphere behavior? *J. Chem. Phys.* 2008, 129(12), 124902.

[54] Poon WCK, Weeks ER, Royall CP. On measuring colloidal volume fractions. *Soft Matter.* 2012, 8(1), 21-30.

[55] Zhuang Y, Charbonneau P. Recent advances in the theory and simulation of model colloidal microphase formers. *J. Phys. Chem. B*. 2016, 120(32), 7775-7782.

[56] Mohanty PS, Paloli D, Crassous JJ, Zaccarelli E, Schurtenberger P. Effective interactions between soft-repulsive colloids: Experiments, theory, and simulations. *J. Chem. Phys.* 2014, 140(9), 094901.

[57] Siebenbürger M, Fuchs M, Ballauff M. Core-shell microgels as model colloids for rheological studies. *Soft Matter.* 2012,8(15), 4014-4024.

[58] Pine DJ, Weitz DA, Zhu JX, Herbolzheimer E. Diffusing-wave spectroscopy: dynamic light scattering in the multiple scattering limit. *J. Phys. France.* 1990, 51(18), 2101-2127.

[59] Nisato G, Hébraud P, Munch JP, Candau SJ. Diffusing-wave-spectroscopy investigation of latex particle motion in polymer gels. *Phys. Rev. E.* 2000, 61(3), 2879.

[60] Durian DJ. Penetration depth for diffusing-wave spectroscopy. *Appl. Opt.* 1995, 34(30), 7100-7105.

[61] Kaplan PD, Kao MH, Yodh AG, Pine DJ. Geometric constraints for the design of diffusing-wave spectroscopy experiments. *Appl. Opt.* 1993, 32(21), 3828-3836.

[62] Dasgupta BR, Tee SY, Crocker JC, Frisken BJ, Weitz DA. Microrheology of polyethylene oxide using diffusing wave spectroscopy and single scattering. *Phys. Rev. E.* 2002, 65(5), 051505.

[63] Viasnoff V, Lequeux F, Pine DJ. Multispeckle diffusing-wave spectroscopy: A tool to study slow relaxation and time-dependent dynamics. *Rev. Sci. Instrum.* 2002, 73(6), 2336-2344.

[64] McKenna GB. Glass dynamics: Diverging views on glass transition. *Nature Phys.* 2008, 4(9), 673.

[65] Viasnoff V, Jurine S, Lequeux F. How are colloidal suspensions that age rejuvenated by strain application? *Faraday Discuss.* 2003, 123(1), 253-266.

[66] Kohlrausch R. Theorie des Elektrischen Rückstandes in der Leidener Flasche. *Ann. Phys.* 1854, 167(2), 179-214.

[67] Williams G, Watts DC. Non-symmetrical dielectric relaxation behavior arising from a simple empirical decay function. *Trans. Faraday Soc.* 1970, 66(1), 80-85.

[68] Ruta B, Chushkin Y, Monaco G, Cipelletti L, Pineda E, Bruna P, Giordano VM, Gonzales-Silveira M. Atomic-Scale Relaxation Dynamics and Aging in a Metallic Glass Probed by X-Ray Photon Correlation Spectroscopy. *Phys. Rev. Lett.* 2012, 109(1), 165701.

[69] Leitner M, Sepiol B, Stadler LM. Time-resolved study of the crystallization dynamics in a metallic glass. *Phys. Rev. B.* 2012, 86(6), 064202.

[70] Ruta B, Baldi G, Monaco G, Chushkin Y. Compressed correlation functions and fast aging dynamics in metallic glasses. *J. Chem. Phys.* 2013, 138(5), 054508.

[71] Cipelletti L, Manley S, Ball RC, Weitz DA. Universal aging features in the restructuring of fractal colloidal gels. *Phys. Rev. Lett.* 2000, 84(10), 2275.

[72] Cipelletti L, Ramos L, Manley S, Pitard E, Weitz DA, Pashkovski EE, Johansson M. Universal non-diffusive slow dynamics in aging soft matter. *Faraday Discuss.* 2003, 123(1), 237-251.

[73] Bandyopadhyay R, Liang D, Harden JL, Leheny RL. Slow dynamics, aging, and glassy rheology in soft and living matter. *Solid State Commun.* 2006, 139(11-12), 589-598.

[74] Czakkel O, Madsen A. Evolution of dynamics and structure during formation of a cross-linked polymer gel. *Europhys. Lett.* 2011, 95(2), 28001.

[75] Knaebel A, Bellour M, Munch JP, Viasnoff V, Lequeux F, Harden JL. Aging behavior of Laponite clay particle suspensions. *Europhys. Lett.* 2000, 52(1), 73.

[76] Bandyopadhyay R, Liang D, Yardimci H, Sessoms DA, Borthwick MA, Mochrie SGJ, Harden JL, Leheny RL. Evolution of particle-scale dynamics in an aging clay suspension. *Phys. Rev. Lett.* 2004, 93(22), 228302.

[77] Ballesta P, Duri A, Cipelletti L. Unexpected drop of dynamical heterogeneities in colloidal suspensions

approaching the jamming transition. *Nat. Phys*. 2008, 4(7), 550.

[78] Caronna C, Chushkin Y, Madsen A, Cupane A. Dynamics of nanoparticles in a supercooled liquid. *Phys. Rev. Lett.* 2008, 100(5), 055702.

[79] Guo H, Bourret G, Corbierre MK, Rucareanu S, Lennox RB, Laaziri K, Piche L, Sutton M, Harden JL, Leheny RL. Nanoparticle motion within glassy polymer melts. *Phys. Rev. Lett.* 2009, 102(7), 075702.

[80] Cipelletti L, Ramos L. Slow dynamics in glassy soft matter. *J. Phys. Condens. Matter.* 2005, 17(6), 253.

[81] Bouchaud JP, Pitard E. Anomalous dynamical light scattering in soft glassy gels. *Eur. Phys. J. E.* 2001, 6(3), 231-236.

[82] Cardinaux F, Cipelletti L, Scheffold F, Schurtenberger P. Microrheology of giant-micelle solutions. *Europhys. Lett.* 2002, 57(5), 738.

[83] Durian DJ, Weitz DA, Pine DJ. Multiple light-scattering probes of foam structure and dynamics. *Science.* 1991, 252(5006), 686-688.

[84] Durian DJ, Weitz DA, Pine DJ. Scaling behavior in shaving cream. *Phys. Rev. A.* 1991, 44(12), 7902.

[85] Sessoms DA, Bissig H, Duri A, Cipelletti L, Trappe V. Unexpected spatial distribution of bubble rearrangements in coarsening foams. *Soft Matter.* 2010, 6(13), 3030-3037.

[86] Tandon P. Effect of stress on the structural relaxation behavior of glasses. *J. Non-Cryst. Solids* 2005, 351(27-29), 2210-2216.

[87] Zhu JX, Pine DJ, Weitz DA. Internal reflection of diffusive light in random media. *Phys. Rev. A.* 1991, 44(6), 3948.

[88] Bellour M, Skouri M, Munch JP, Hébraud P. Brownian motion of particles embedded in a solution of giant micelles. *Eur. Phys. J. E.* 2002, 8(4), 431-436.

[89] Menon N, Durian DJ. Diffusing-wave spectroscopy of dynamics in a three-dimensional granular flow. *Science.* 1997, 275(5308), 1920-1922.

[90] Del Gado E, Kob W. Length-Scale-Dependent Relaxation in Colloidal Gels. *Phys. Rev. Lett.* 2007, 98(2), 028303.

[91] Bouzid M, Colombo J, Barbosa LV, Del Gado E. Elastically driven, intermittent microscopic dynamics in soft solids. *Nature Commun.* 2017, 8(1), 15846.

[92] Chremos A, Douglas JF. Particle localization and hyperuniformity of polymer-grafed nanoparticle materials. *Ann. Phys. (Berlin)* 2017, 529(5), 1600342.

[93] Douglas JF. Internal communications.

[94] Morishita T. Compressed exponential relaxation in liquid silicon: Universal feature of the crossover from ballistic to diffusive behavior in single-particle dynamics. *J. Chem. Phys.* 2012, 137(2), 024510.

[95] Seo JA, Kwon HJ, Kataoka K, Ohshima KI, Shin DM, Kim HK, Hwang YH. Compressed-exponential relaxations in supercooled liquid trehalose. *Cur. Appl. Phys.* 2012, 12(6), 1548-1552.

[96] Allegrini P, Douglas JF, Glotzer SC. Dynamic entropy as a measure of caging and persistent particle

motion in supercooled liquids. *Phys. Rev. E.* 1999, 60(5), 5714.

[97] Heussinger C, Berthier L, Barrat JL. Superdiffusive, heterogeneous, and collective particle motion near the fluid-solid transition in athermal disordered materials. *Europhys. Lett.* 2010, 90(2), 20005.

[98] McKenna GB. Mechanical rejuvenation in polymer glasses: fact or fallacy? *J. Phys. Condens. Matter.* 2003, 15(11), S737.

[99] Sánchez-Díaz LE, Ramírez-González PE, Medina-Noyola M. Equilibration and aging of dense soft-sphere glass-forming liquids. *Phys. Rev. E.* 2013, 187(5), 052306.

[100] Sánchez-Díaz LE, Lázaro-Lázaro E, Olais-Govea JM, Medina-Noyola M. Non-equilibrium dynamics of glass-forming liquid mixtures. *J. Chem. Phys.* 2014, 140(23), 234501.

[101] Schoenholz SS, Cubuk ED, Sussman DM, Kaxiras E, Liu AJ. A structural approach to relaxation in glassy liquids. *Nat. Phys.* 2016, 12(5), 469.

[102] Gabriel J, Blochowicz T, Stühn B. Compressed exponential decays in correlation experiments: The influence of temperature gradients and convection. *J. Chem. Phys.* 2015, 142(10), 104902.

Graphical Table of Contents.

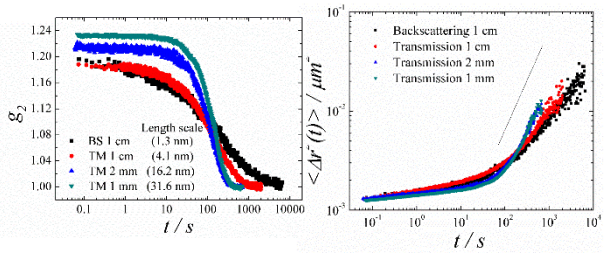

Physical Aging and Compressed Exponential Behaviors in a Model Soft Colloidal System

Qi Li, Xiaoguang Peng, and Gregory B. McKenna

Compressed exponential $g_2(t)$ does not require super-diffusive MSD behavior.